

Learning to Imagine Manipulation Goals for Robot Task Planning

Chris Paxton¹, Kapil Katyal¹, Christian Rupprecht², Raman Arora¹, Gregory D. Hager¹

Abstract—Prospection is an important part of how humans come up with new task plans, but has not been explored in depth in robotics. Predicting multiple task-level is a challenging problem that involves capturing both task semantics and continuous variability over the state of the world. Ideally, we would combine the ability of machine learning to leverage big data for learning the semantics of a task, while using techniques from task planning to reliably generalize to new environment. In this work, we propose a method for learning a model encoding just such a representation for task planning. We learn a neural net that encodes the k most likely outcomes from high level actions from a given world. Our approach creates comprehensible task plans that allow us to predict changes to the environment many time steps into the future. We demonstrate this approach via application to a stacking task in a cluttered environment, where the robot must select between different colored blocks while avoiding obstacles, in order to perform a task. We also show results on a simple navigation task. Our algorithm generates realistic image and pose predictions at multiple points in a given task.

I. INTRODUCTION

How can we allow robots to plan as humans do? Humans are masters at solving problems. When attempting to solve a difficult problem, we can picture what effects our actions will have, and what the consequences will be. Some would say this act — the act of prospection — is the essence of intelligence [?].

Consider the task of stacking a series of colored blocks in a particular pattern as explored in prior work [1], [2]. A traditional planner would view this as a sequence of high-level actions, such as `pickup(block)`, `place(block, on_block)`, and so on. The planner will then decide which object gets picked up and in which order. Such tasks are often described using a formal language such as the Planning Domain Description Language (PDDL) [3]. To execute such a task on a robot, specific goal conditions and cost functions must be defined, and the preconditions and effects of the each action must be specified – which is a large and time consuming undertaking [4]. Humans, on the other hand, do not require that all of this information be given beforehand. We can learn models of task structure purely from observation or demonstration. We work directly with high dimensional data such as images, and can reason over complex paths without being given an explicit structure.

As a result, there has been much interest in learning prospective models for planning and action. Deep generative

models such as conditional GANS [5] or multiple-hypothesis models for image prediction [6], [7] allow us to generate realistic future scenes. In addition, a recent line of work in robotics focuses on making structured prediction [8], [9]; [10] proposed SE3-nets, which predict object motion masks and six degree of freedom movement for each object; [11] predict trajectories to move to intermediate goals. However, so far these approaches focus on making relatively short-term predictions, and do not take into account variability in the ways a task can be performed in a stochastic world.

In general, deep policy learning has proven successful at learning well-scoped, short horizon robotic tasks [12], [13], [9]. Recent work on one-shot imitation learning learned general-purpose models for manipulating blocks, but relies on a task solution from a human expert and does not generate prospective future plans for reliable performance in new environments [1], [2]. These are very data intensive as a result: [1] used 140,000 demonstrations.

Instead, we propose a model that learns this high level task structure and uses it to generate interpretable task plans by predicting sequences of movement goals. These movement goals can then be connected via traditional trajectory optimization or motion planning approaches that can operate on depth data without a semantic understanding of the world. Fig. 1 shows the task as well as predictions resulting from our algorithm at different stages.

To summarize, our contributions are:

- Approach for learning a predictive model over world state transitions from a large supervised dataset, suitable for task planning.
- Analysis of the parameters that make such learning feasible in a stochastic world.
- Experimental results from a simulated navigation and a block-stacking domain.

II. RELATED WORK

In robotics, TAMP approaches are very effective at solving complex problems involving spatial reasoning [14], [15]. A subset of planners focused on Partially Observed Markov Decision Process extend this capability into uncertain worlds, such as DeSPOT [16]. Only a few recent works have explored integration of planning and learning. Recent work has examined combining these approaches with QMDP-nets [17] that embed learning into a planner using a combination of a filter network and a value function approximator network in the form of a set of convolutional layers with shared weights. Similarly, value iteration networks embed a planner into a neural network which can learn navigation tasks [18]. [19]

¹Department of Computer Science, The Johns Hopkins University, Baltimore, MD, USA. Email: cpaxton@jhu.edu, kkatyal2@jhu.edu, hager@cs.jhu.edu, arora@cs.jhu.edu

²Technical University of Munich, Munich, Bavaria, Germany. Email: christian.rupprecht@in.tum.de

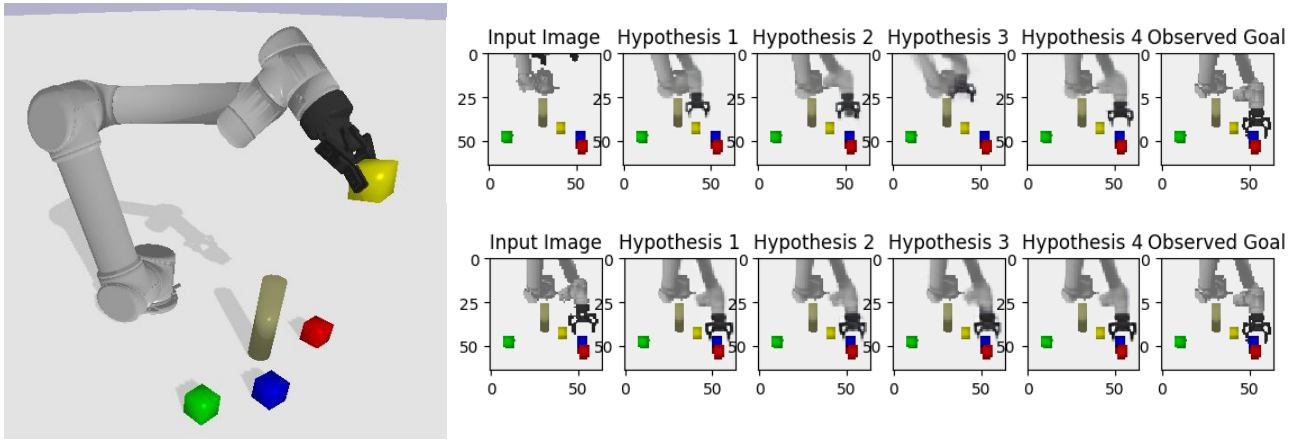


Fig. 1: A simple stacking task including an obstacle that must be avoided. The robot must decide which blocks to pick up and move, and which block to put them on, taking into account its workspace and the obstacle. The right side shows how predictions change as the robot moves.

discuss neural network architectures for memory in navigation. [20] propose the Strategic Attentive Writer (STRAW) as a sequence prediction technique applicable to planning sequences of actions. In [21] the authors use Monte Carlo Tree Search (MCTS) together with a set of learned action and control policies, but again do not learn a predictive model of the future. However, none of these approaches provide a way to predict or evaluate possible futures.

In this work, we examine the problem of learning representations for high-level predictive models for task planning. Prediction is intrinsic to planning in a complex world [?]. Robotic motion planners assume a causal model of the world. [22] fit a predictive model to predict the true state of an occluded world as it evolves over time. [23] propose PredNet as a way of predicting sequences of images from sensor data, likewise with the goal being to predict the future. [9] use unsupervised learning of visual models to push objects around in a plane.

The options framework provides a way to think of MDPs as a set of many high level “options,” each active over a certain window [24]. Policy sketches [25] are one method that uses curriculum learning with a set of “policy sketches.” Another option is FeUdal networks, in which a “manager” network sets goals for lower level “worker” networks [26].

a) Learning Generative Models.: Such a prediction system must be able to deal with a stochastic world. Prior work has examined several ways of generating multiple realistic predictions [6], [7], [11]. Generative Adversarial Networks (GANs) can be used to generate samples as well. [27] applied adversarial methods to imitation learning. [6] proposed a multiple hypothesis loss function as a way of predicting multiple possible goals when the prediction task is ambiguous. Similarly, [7] proposed a custom loss to synthesize a diverse collection of photorealistic images. [8] learn a deep autoencoder as a set of convolutional blocks followed by a spatial softmax; they find that this representation is useful for reinforcement learning. More recently, [11] proposed to learn a deep predictive network

that uses a stochastic policy over goals for manipulation tasks, but without the goal of additionally predicting the future world state. [13] learn a deep multimodal embedding for a variety of tasks; this representation allows them to adapt to appliances with different interfaces while reasoning over trajectories, natural language descriptions, and point clouds for a given task. Recently, [28] propose DARLA, the Disentangled Representation Learning Agent, which learns useful representations for tasks that enable generalization to new environments.

III. APPROACH

We define a planning problem with continuous states $x \in \mathcal{X}$ and controls $u \in \mathcal{U}$. Here, x contains observed information about the world: for example, for a manipulation task, it includes the robot’s end effector pose and input from a camera viewing the scene. We augment this with high-level actions $a \in \mathcal{A}$ that describe the task structure. We also assume that there is some hidden world state h , which encodes both task information and the underlying truth of the input from the various sensors. The symbolic world state here is not observed directly: there are numerous possible combinations of predicates that could be meaningful.

Our goal is to learn models grounding this problem as an MDP over options, so that at run time we can generate intelligent, comprehensible task plans. Specifically, we will first learn a goal prediction function, which is a mapping $T(x, a) \rightarrow (x', a)$. In other words, given a particular action and an observed prediction, we want to be able to predict both a continuous end goal and the actions necessary to take us there.

We posit three components of this goal prediction function:

1. $f_{enc}(x, a) \rightarrow h$, a learned encoder function maps observations and descriptions to the hidden state.
2. $f_{dec}(h) \rightarrow (x, a)$, a decoder function that maps from the hidden state of the world to the observation space.

- $T_i(h) \rightarrow h'$, the i -th learned world state transformation function, which maps to different positions in the space of possible hidden world states.

In addition, we assume that the hidden state h consists of all the necessary information about the world. As such, we can learn two additional functions of use in planning:

- $V(h)$, the expected reward-to-go from a particular hidden state
- $p(a|h)$, the policy over discrete high-level actions from a given hidden state

While we cannot observe the hidden world state, we can observe all of these other fields easily, given demonstrations of a task. Prior work has examined learning feature encoding [29], [30]. Our goal is to learn a set of encoders and decoders that project our available features into the latent world state h that can be used for planning.

Our method assumes we have a dataset, containing mixed execution failures and successes, where we wish to be able to predict a large number of plausible task executions and their consequences. We generate a large data set of action executions, with mid- and high-level labels. We assume semantic labels have been provided for different actions to provide meaningful intermediate goals for prediction, such as `grasp(red_block)` or `close_gripper`.

A. Model Architecture

Fig. 2 shows the architecture of our subtask goal prediction network. The model takes in the observed high-level action a and the state observations x . For the manipulator example, $x = (x_I, x_{ee}, x_g)$ is the image, arm position, and gripper state, respectively; for the navigation task, $x = (x_I, x_p)$ is the image and the robot’s position in the world.

The encoder $f_{enc}(x)$ is a set of 5×5 convolutional blocks. After the first convolution with stride 1, we tile input from the robot’s measured state (end effector pose or robot position) as additional information. The last layers in the network are a set of spatial soft-argmax layers, as used by [8], [11] and [31]. These layers extract a set of keypoints which form our “hidden” representation to be fed into the Transform block. Each Transform block is composed of a set of dense layers.

We examine two alternative models for our neural network architecture: a simple encoder-decoder neural network and a U-net. The U-net is similar to the model proposed by [5] for image generation using conditional Generative Adversarial Networks, and was found to generate very realistic images when performing photographic image synthesis [7].

The nonlinear transformation function $T_j(h) \rightarrow h'$ maps the current hidden world representation h to one of the m latent representations h'_j that represent possible goals the robot could pursue. We can then select between available goals to generate a task plan. This is beneficial since predicting a future state from x is an ambiguous problem; we can allow the system to predict several possible hypotheses h'_j from the current state h . Since in the training data for every roll out of the task we only see one possible future instead of all

of them, we need to take special care of training the system to allow it to predict multiple possibilities. This is achieved through the multiple hypotheses loss described in Sec. III-B.

Finally, in most tasks, there is some variability over specific goal poses. In order to generate crisp, reliable hypotheses, we consider representing this variability by concatenate a vector of random noise at every step in the training process to the hidden state, before applying the transformations, with the goal being to represent the minor variability between actions. In this case, the transformation function would be expressed as $T_j(h, z)$ for a uniformly-sampled random noise vector z .

B. Multiple Hypotheses Loss Function

Many deep learning approaches fail when learning approaches for which there are multiple, disjoint correct outputs. For this reason, recent work has explored multiple hypothesis learning for prediction [6] and for photographic image generation [7]. We use a modified version of the Multiple Hypothesis (MHP) loss function [6] to train our predictor model. This will predict $N_H = 4$ to $N_H = 8$ different possible future worlds.

The loss for a single hypothesis \hat{x}_i is expressed as the weighted sum of the different outputs, where each state x is expressed as a number of different observation variables v , each of which is some subset of this observed state x . For example, with the manipulator robot, $v \in \{I, q, g\}$ is one of our three classes of observations available based on the robot’s current state. For a mobile robot x may consist of GPS position and camera view. This means that for a particular hypothesis \hat{x}_i , the loss $c(\cdot, \cdot)$ is expressed as:

$$c(\hat{x}_i, \hat{a}_i) = w_a c(a) + \sum_{v \in x} w_v c(\hat{v}_i).$$

Here w_v is the weight associated with a particular view of the world state, and w_a is the weight associated with predicting the correct low-level action. In practice, we use $c(x_i) = \|x_i - \hat{x}_i\|$, the mean absolute error (MAE), when computing the loss on predicted state variables. The MAE encourages the system to make as few mistakes as possible when predicting these errors, and has a normalizing effect that reduces small errors. This results in sharper predictions in practice. We handle high-level action predictions \hat{a} slightly differently. We use an embedding for the action description to map it to a one-hot vector, and compute the cross entropy loss based on $p(a')$.

Then, we can express the loss function simply as:

$$c(x, a) = \min_i c(\hat{x}_i, \hat{a}_i).$$

The issue with this is that in many cases some hypotheses will not make sense. To deal with this, we consider adding an exploration probability λ , such that with uniform probability we select one of the existing hypotheses to update. This is equivalent to adding an average cost to the existing loss function. Thus, the overall loss is computed as:

$$(1 - \lambda) \min_i c(\hat{x}_i, \hat{a}_i) + \frac{\lambda}{N_H} \sum_i^{N_H} c(\hat{x}_i, \hat{a}_i).$$

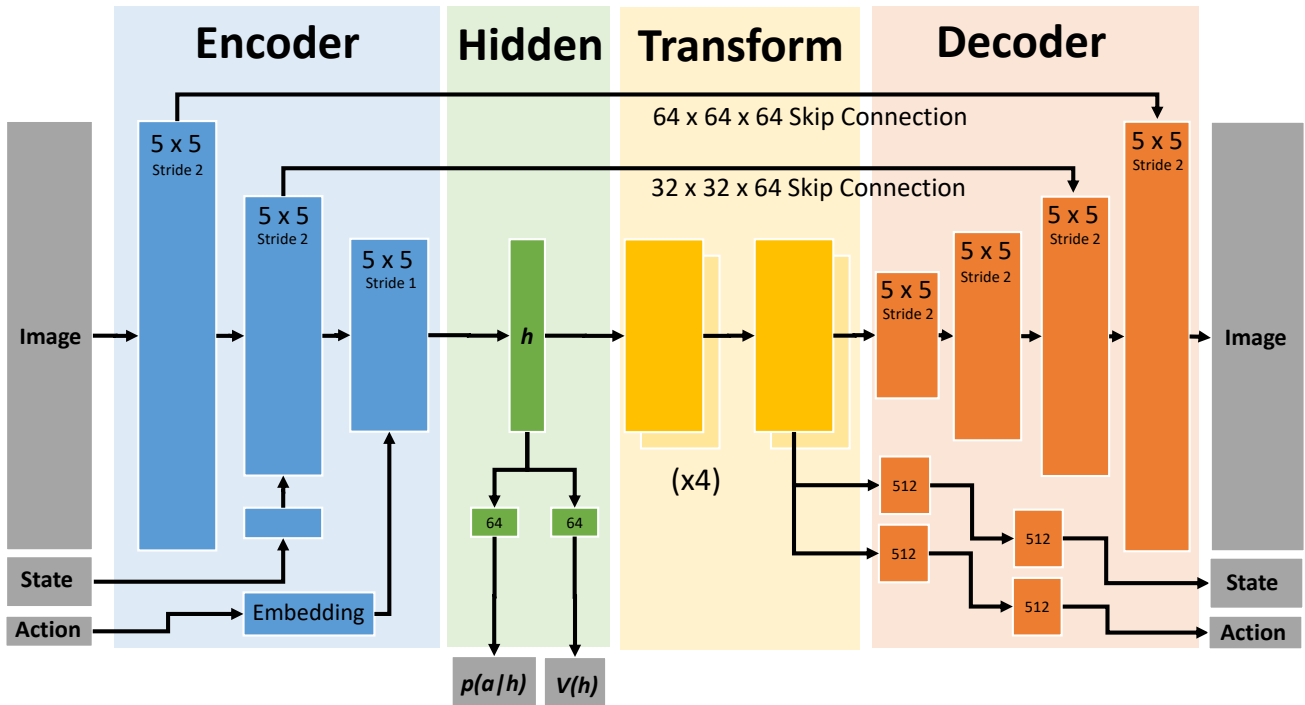


Fig. 2: Overview of the predictor network. The input image and features are passed through a series of convolutional blocks in the Encoder and a spatial softmax extracts the hidden state representation. The dense layers in the Transform block compute a new world state, which is the input into the Decoder network.

We used $N_H = 4$ hypotheses in our experiments, with $\lambda = 0.05$.

C. Value Function and Action Prior

In addition, we learn two functions $V(h)$ and $p(a|h)$. These are the estimated value of a given world, and the probability of taking a particular action from that world, respectively. The value function $V(h)$ is trained using the full data set, and can be learned end-to-end with the encoder-transform-decoder architecture. The value function operates on the current hidden state h and returns the expected reward-to-go – i.e. whether or not we expect to see a possible success or failure farther on in the task if we continue down this route.

The action prior $p(a|h)$ is learned on successful training data only. The goal of this function is to tell us which actions to explore first, when performing a tree search over different possible futures. This is useful because performing a tree expansion is a relatively expensive process. We also provide this action prior as an additional input to the transform block.

IV. EXPERIMENTAL SETUP

We applied the proposed method to both a simple navigation task using a simulated Husky robot, and to a UR5 block-stacking task.¹

In all examples, we follow a simple process for collecting data. First, we generate a random world configuration, determining where objects will be placed in a given scene.

¹Source code for all examples will be made available after publication.

The robot is initialized in a random pose as well. We automatically build a task model that defines a set of control laws and termination conditions, which are used to generate the robot motions in the set of training data. Legal paths through this task model include any which meet the high-level task specification, but may still violate constraints (due to collisions or errors caused by stochastic execution).

We include both positive and negative examples in our training data. Training was performed with Keras [32] and Tensorflow for 30,000 iterations on an NVidia Tesla K80 GPU, with a batch size of 32. Training took 12-18 hours, depending on the exact parameters used.

A. Robot Navigation

In the navigation task, we modeled a Husky robot moving through a construction site environment. The high level actions available to the robot are to investigate one of four objects: a barrel, a barricade, a construction pylon or a block. We represent the robot state by the six Degree of Freedom (6DOF) pose of the robot, represented as the concatenation of position (x, y, z) and orientation $(\omega_r, \omega_p, \omega_y)$. In addition to the robot state, we use a 64x64 RGB image taken from overhead of the scene to provide an aerial view of the environment. Data was collected using a Gazebo simulation of the robot navigating to any of the four targets. We trained the network from Fig. 2 to generate predictions of these possible goals with the number of hypotheses set to 4.

Fig. 3 shows examples of the robot in its start and (ground truth) goal pose, as well as 4 hypothetical future predictions

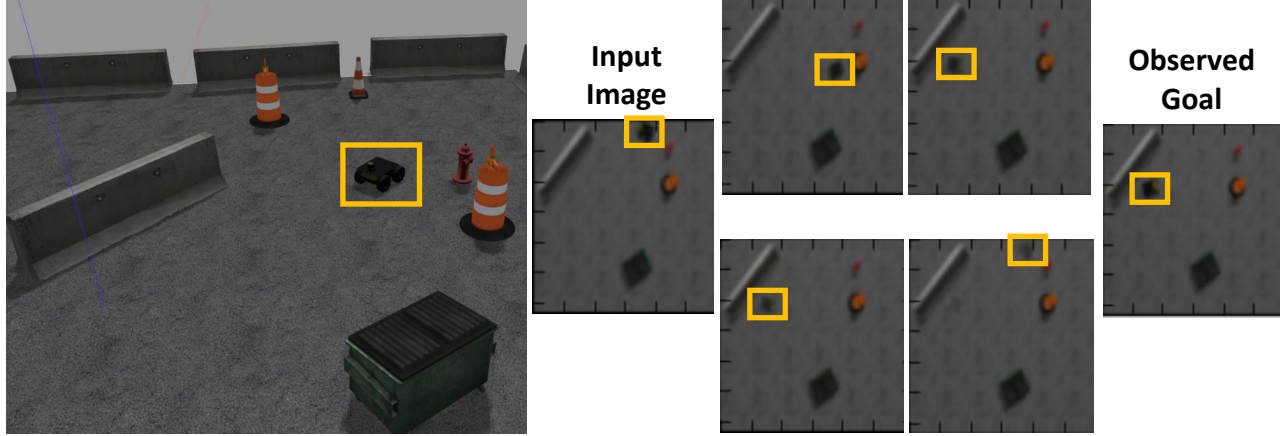


Fig. 3: Prediction Results from Husky Simulation. Image on the left shows the scene in the Gazebo simulator; right images show predicted possible destinations. Robot position is highlighted.

generated from the dataset. The robot was able to accurately predict input images to the same fidelity as the input image. We also analyzed the effect of varying network architectures on the final pose error prediction.

B. Block Stacking

To analyze our ability to predict goals for task planning, we learn in a more elaborate environment. In the block stacking task, the robot needed to pick up a colored block and place it on top of any other colored block. To add difficulty, we place a single obstacle in the world. The robot succeeds if it manages to stack any two blocks on top of one another and failed immediately if either it touches this obstacle or if at the end of 30 seconds the task has not been achieved. Training was performed on a relatively small number of examples: we used 7500 trials, of which 3152 were successful.

In this case, we represent the robot in terms of its 6DOF end effector pose x_{ee} , encoded as the concatenation of the position (x, y, z) and the roll-pitch-yaw $(\omega_r, \omega_p, \omega_y)$, such that $x_{ee} = \{x, y, z, \omega_r, \omega_p, \omega_y\}$. The state of the gripper was expressed as a single variable $x_g \in (0, 1)$. In addition, we provide a 64×64 RGB image of the scene from an external camera, referred to as x_I . Fig. 1 shows the results of this process. Scenes included four blocks and the obstacle in addition to the robot, but lack any other objects or background clutter.

V. RESULTS

Fig. 1 shows examples of good predictions in at two different points in the block-stacking task: when first choosing a block to pick up, and lifting the block over the obstacle. Our model attempts to predict both failures and successes, but we see far better accuracy when predicting successes on our data set due to high variability in possible failures. Fig. 4. shows the robot attempting to pick up red block, but the blue block interfered. This will result in a task failure, which means the robot should attempt to pick up a different block first instead.

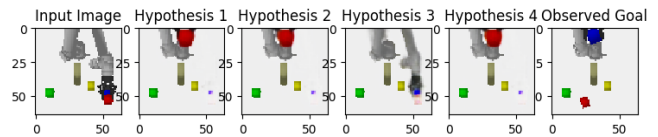


Fig. 4: An example of a bad prediction. Here, the algorithm clearly attempts to predict what happens when it picks up the red block, but the blue block prevented the gripper from properly closing.

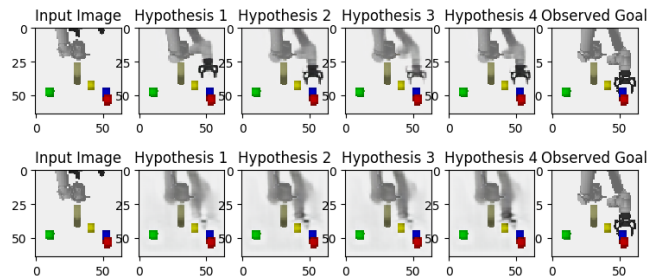


Fig. 5: Predictions made using different levels of dropout to train the decoder network. On the top, the decoder was trained with a dropout rate of 0.125; on the bottom, the network was trained with dropout of 0.5.

Such failures are random and hard to predict, in contrast to successes which tend to be very similar.

a) *Dropout and Stochastic Predictions.*: Differing levels of dropout have a marked effect on the quality of the models learned during our training process. Compare the set of predictions on the top of Fig. 5 with those on the bottom, versus those in Fig. 6.

Using dropout in either the transforms or in the decoder will blur the results, giving us a less accurate estimate of what the future world may look like. Using insufficient dropout will likewise cause issues, because of the high

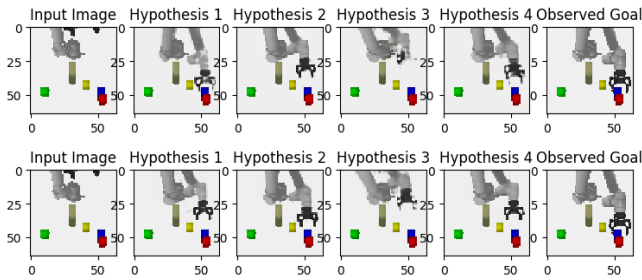


Fig. 6: Concatenating a vector of random noise to the image allows individual transforms to better capture uncertainty in the resulting image. This results in crisper predicted images (bottom).

accumulated variance between objects over time.

We provide a different random seed at each time step for each prediction; the networks are able to use this noise during execution to capture some additional level of uncertainty. A dropout level of 0.125 – 0.25 provided the best results; for future versions of the model, we use these dropout levels.

b) Representing Randomness.: We represent randomness in two ways: (1) as the discrete choice of which hypothesis occurs, and (2) as a vector of additional noise concatenated to the hidden representation. We find that both of these are useful for representing randomness in the resulting world state, in a way that gives us relatively crisp, realistic images.

Fig. 6 shows the effect on models with no dropout. On the top we see a model trained without this random vector; on the bottom we see one trained with it. The addition of random noise allows the model to generate cleaner predictions. Our results show that capturing randomness may help learning predictive task models, but results are somewhat inconclusive: on training experiments with a large amount of dropout, these made little difference. With relatively low levels of dropout (e.g. dropout of 0.125), we saw that adding a 32-D noise vector resulted in validation loss of 0.0125 vs. 0.0150 when including negative examples, though we did not observe the same effect with higher levels of dropout. This sort of randomness makes a small difference under different conditions, and led to better generalization and improved test performance. Adding 32 random noise dimensions to our final model saw image loss of 1.21×10^{-4} and pose error of 5.51×10^{-5} after 300,000 training steps, while not adding this random noise had a comparable image loss (1.85×10^{-4}) but a noticeably higher average pose error on test data (8.60×10^{-5}). These findings suggest that adding this vector is unimportant for “big picture” details, but that it helps capture small, local variance.

We compared against one additional method for representing randomness within each mode: predicting a mean and a covariance for each transform, which necessitated adding a KL loss term to the proposed loss. However, this resulted both in worse performance and resulted in the collapse of the separate modes.

c) Skip Connections.: We compare the error of our models both with and without skip connections between the encoder and the image decoder. This version of the model was trained and evaluated on successful trials. Fig. 7 shows an example of results without skip connections: the model was able to learn several possible positions, but image quality is subjectively far lower.

In addition, we compared absolute image and pose error for models trained with and without training data on both versions of the model. We see that without skip connections, we see an image-pixel error of 5.01×10^{-4} , with an average pose error of 9.61×10^{-5} . Total, weighted validation loss was 0.012. By contrast, for the version with skip connections, we see image loss of 1.21×10^{-4} and pose error of 5.51×10^{-5} . In short, we can see that the skip connections make a difference when it comes to image reconstruction: images are both qualitatively higher quality, and have a quarter the pixel-wise error. In addition, end effector poses are roughly twice as accurate.

Presumably, a large part of the advantage of skip connections is that the hidden state only needs to encode aspects of the image that are changing from one frame to the next. Fig. 7 (right) shows the effect this has on training: loss remained consistently higher for the version without skips.

VI. CONCLUSIONS

We described an approach for learning a predictive model that can be used to generate interpretable task plans for robot execution. This model supports complex tasks, and requires only minimal labeling. It can also be applied to many different domains with minimal adaptation. We also provided an analysis of how to create and train models for this problem domain, and describe the validation of the final model architecture in a range of different domains.

Still, there are clear avenues for improvement in future work. First, in this work we assume that low-level “actor” policies are provided. This is sufficient for most manipulation and navigation tasks, but may not capture complex object interactions. Second, we assume the existence of mid-level supervisory labels in this work to extract change-points. In the future, we would prefer to detect change-points automatically using an approach such as that proposed by [33]. Finally, we plan to expand this method into a full planning algorithm using predicted value and action priors that operates on sensor data.

REFERENCES

- [1] Y. Duan, M. Andrychowicz, B. Stadie, J. Ho, J. Schneider, I. Sutskever, P. Abbeel, and W. Zaremba, “One-shot imitation learning,” *arXiv preprint arXiv:1703.07326*, 2017.
- [2] D. Xu, S. Nair, Y. Zhu, J. Gao, A. Garg, L. Fei-Fei, and S. Savarese, “Neural task programming: Learning to generalize across hierarchical tasks,” *arXiv preprint arXiv:1710.01813*, 2017.
- [3] M. Ghallab, C. Knoblock, D. Wilkins, A. Barrett, D. Christianson, M. Friedman, C. Kwok, K. Golden, S. Penberthy, D. E. Smith, *et al.*, “PDDL—the planning domain definition language,” <http://www.citeulike.org/group/13785/article/4097279>, 1998.
- [4] M. Beetz, D. Jain, L. Mosenlechner, M. Tenorth, L. Kunze, N. Blodow, and D. Pangercic, “Cognition-enabled autonomous robot control for the realization of home chore task intelligence,” *Proceedings of the IEEE*, vol. 100, no. 8, pp. 2454–2471, 2012.

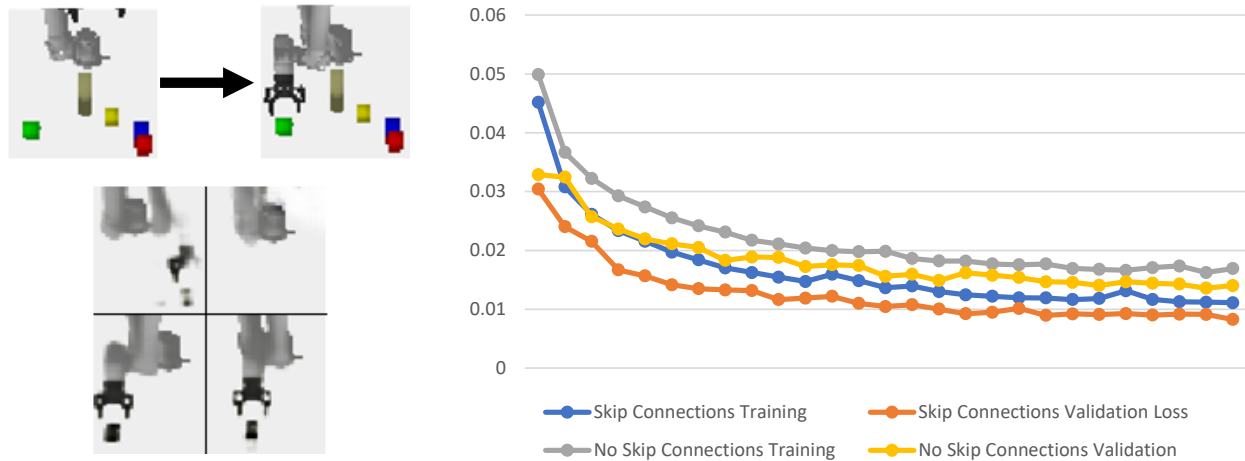


Fig. 7: Without the skip connections, the model has a harder time learning what aspects of the scene are important and which will change over time. Left: example of images produced with no skip connections. Right: training and validation loss for the first 7,500 iterations.

[5] P. Isola, J. Zhu, T. Zhou, and A. A. Efros, "Image-to-image translation with conditional adversarial networks," *CoRR*, vol. abs/1611.07004, 2016. [Online]. Available: <http://arxiv.org/abs/1611.07004>

[6] C. Rupprecht, I. Laina, R. DiPietro, M. Baust, F. Tombari, N. Navab, and G. D. Hager, "Learning in an uncertain world: Representing ambiguity through multiple hypotheses," *International Conference on Computer Vision (ICCV)*, 2017.

[7] Q. Chen and V. Koltun, "Photographic image synthesis with cascaded refinement networks," *arXiv preprint arXiv:1707.09405*, 2017.

[8] C. Finn, X. Y. Tan, Y. Duan, T. Darrell, S. Levine, and P. Abbeel, "Deep spatial autoencoders for visuomotor learning," in *Robotics and Automation (ICRA)*, 2016 *IEEE International Conference on*. IEEE, 2016, pp. 512–519.

[9] C. Finn, I. Goodfellow, and S. Levine, "Unsupervised learning for physical interaction through video prediction," in *Advances in Neural Information Processing Systems*, 2016, pp. 64–72.

[10] A. Byravan and D. Fox, "Se3-nets: Learning rigid body motion using deep neural networks," in *Robotics and Automation (ICRA)*, 2017 *IEEE International Conference on*. IEEE, 2017, pp. 173–180.

[11] A. Ghadirzadeh, A. Maki, D. Kragic, and M. Björkman, "Deep predictive policy training using reinforcement learning," *arXiv preprint arXiv:1703.00727*, 2017.

[12] S. Levine, C. Finn, T. Darrell, and P. Abbeel, "End-to-end training of deep visuomotor policies," *Journal of Machine Learning Research*, vol. 17, no. 39, pp. 1–40, 2016.

[13] J. Sung, S. H. Jin, I. Lenz, and A. Saxena, "Robobarista: Learning to manipulate novel objects via deep multimodal embedding," *arXiv preprint arXiv:1601.02705*, 2016.

[14] F. Lagriffoul, D. Dimitrov, J. Bidot, A. Saffiotti, and L. Karlsson, "Efficiently combining task and motion planning using geometric constraints," *The International Journal of Robotics Research*, p. 0278364914545811, 2014.

[15] M. Toussaint, "Logic-geometric programming: An optimization-based approach to combined task and motion planning," in *International Joint Conference on Artificial Intelligence*, 2015.

[16] A. Somani, N. Ye, D. Hsu, and W. S. Lee, "Despot: Online pomdp planning with regularization," in *Advances in neural information processing systems*, 2013, pp. 1772–1780.

[17] P. Karkus, D. Hsu, and W. S. Lee, "Qmdp-net: Deep learning for planning under partial observability," *arXiv preprint arXiv:1703.06692*, 2017.

[18] A. Tamar, Y. Wu, G. Thomas, S. Levine, and P. Abbeel, "Value iteration networks," in *Advances in Neural Information Processing Systems*, 2016, pp. 2154–2162.

[19] S. W. Chen, N. Atanasov, A. Khan, K. Karydis, D. D. Lee, and V. Kumar, "Neural network memory architectures for autonomous robot navigation," *arXiv preprint arXiv:1705.08049*, 2017.

[20] A. Vezhnevets, V. Mnih, S. Osindero, A. Graves, O. Vinyals, J. Agapiou, et al., "Strategic attentive writer for learning macro-actions," in *Advances in Neural Information Processing Systems*, 2016, pp. 3486–3494.

[21] C. Paxton, V. Raman, G. D. Hager, and M. Kobilarov, "Combining neural networks and tree search for task and motion planning in challenging environments," *CoRR*, vol. abs/1703.07887, 2017. [Online]. Available: <http://arxiv.org/abs/1703.07887>

[22] P. Ondruska and I. Posner, "Deep tracking: Seeing beyond seeing using recurrent neural networks," *arXiv preprint arXiv:1602.00991*, 2016.

[23] W. Lotter, G. Kreiman, and D. Cox, "Deep predictive coding networks for video prediction and unsupervised learning," *arXiv preprint arXiv:1605.08104*, 2016.

[24] R. S. Sutton, D. Precup, and S. Singh, "Between mdps and semi-mdps: A framework for temporal abstraction in reinforcement learning," *Artif. Intell.*, vol. 112, no. 1-2, pp. 181–211, Aug. 1999. [Online]. Available: [http://dx.doi.org/10.1016/S0004-3702\(99\)00052-1](http://dx.doi.org/10.1016/S0004-3702(99)00052-1)

[25] J. Andreas, D. Klein, and S. Levine, "Modular multitask reinforcement learning with policy sketches," *arXiv preprint arXiv:1611.01796*, 2016.

[26] A. S. Vezhnevets, S. Osindero, T. Schaul, N. Heess, M. Jaderberg, D. Silver, and K. Kavukcuoglu, "Feudal networks for hierarchical reinforcement learning," *arXiv preprint arXiv:1703.01161*, 2017.

[27] J. Ho and S. Ermon, "Generative adversarial imitation learning," in *Advances in Neural Information Processing Systems*, 2016, pp. 4565–4573.

[28] I. Higgins, A. Pal, A. A. Rusu, L. Matthey, C. P. Burgess, A. Pritzel, M. Botvinick, C. Blundell, and A. Lerchner, "Darla: Improving zero-shot transfer in reinforcement learning," *arXiv preprint arXiv:1707.08475*, 2017.

[29] R. Parr, L. Li, G. Taylor, C. Painter-Wakefield, and M. L. Littman, "An analysis of linear models, linear value-function approximation, and feature selection for reinforcement learning," in *Proceedings of the 25th international conference on Machine learning*. ACM, 2008, pp. 752–759.

[30] Z. Song, R. E. Parr, X. Liao, and L. Carin, "Linear feature encoding for reinforcement learning," in *Advances in Neural Information Processing Systems*, 2016, pp. 4224–4232.

[31] S. Levine, C. Finn, T. Darrell, and P. Abbeel, "End-to-end training of deep visuomotor policies," *arXiv preprint arXiv:1504.00702*, 2015.

[32] F. Chollet, "Keras," <https://github.com/fchollet/keras>, 2015.

[33] S. Niekum, S. Osentoski, G. Konidaris, and A. G. Barto, "Learning and generalization of complex tasks from unstructured demonstrations," in *Intelligent Robots and Systems (IROS)*, 2012 *IEEE/RSJ International Conference on*. IEEE, 2012, pp. 5239–5246.